

## Stabilization of $\text{Sn}^{2+}$ in $\text{K}_{10}\text{Sn}_3(\text{P}_2\text{Se}_6)_4$ and $\text{Cs}_2\text{SnP}_2\text{Se}_6$ Derived from a Basic Flux

In Chung and Mercouri G. Kanatzidis\*

Department of Chemistry, Northwestern University, Evanston, Illinois 60208, United States

Received June 6, 2010

$\text{K}_{10}\text{Sn}_3(\text{P}_2\text{Se}_6)_4$  and  $\text{Cs}_2\text{SnP}_2\text{Se}_6$  stabilize the lower oxidation state of  $\text{Sn}^{2+}$ .  $\text{K}_{10}\text{Sn}_3(\text{P}_2\text{Se}_6)_4$  crystallizes in the trigonal space group  $R\bar{3}$  with  $a = b = 24.1184(7)$  Å and  $c = 7.6482(2)$  Å at 100 K.  $\text{Cs}_2\text{SnP}_2\text{Se}_6$  crystallizes in  $P2_1/c$  with  $a = 10.1160(4)$  Å,  $b = 12.7867(5)$  Å,  $c = 11.0828(5)$  Å, and  $\beta = 94.463(3)^\circ$  at 100(2) K. Electronic absorption spectra revealed band gaps of 1.82 eV for  $\text{K}_{10}\text{Sn}_3(\text{P}_2\text{Se}_6)_4$  and 2.06 eV for  $\text{Cs}_2\text{SnP}_2\text{Se}_6$ . Solid-state magic-angle-spinning  $^{31}\text{P}$  NMR, UV–vis, Raman, and IR spectroscopy and thermal analysis studies of the compounds are reported.

Chalcophosphates are ternary (M/P/Q) and quaternary (A/M/P/Q) compounds with  $[\text{P}_x\text{Q}_y]^{n-}$  anions in their structure, where M is a metal, A is an alkali metal, and Q is sulfur or selenium. This class of compounds is attractive for investigation because many of its members exhibit technologically important properties such as large optical nonlinearities,<sup>1</sup> reversible redox chemistry relevant to secondary batteries,<sup>2</sup> and photoluminescence,<sup>3</sup> ferroelectric,<sup>4</sup> and phase-change properties.<sup>5</sup> The molten salt method is a powerful tool for the

discovery of chalcophosphate compounds<sup>6</sup> because anionic  $[\text{P}_x\text{Q}_y]^{n-}$  units form in these fluxes and behave as versatile ligands that bind to metal cations. The control of the starting compositions allows for a very adaptable chemistry by means of controlling the stabilization and concentration of the various  $[\text{P}_x\text{Q}_y]^{n-}$  building blocks. The application of this flux method to tin at intermediate reaction temperatures (300–500 °C) gave unusual compounds such as  $\text{A}_5\text{Sn}(\text{PSe}_5)_3$  (A = K, Rb),  $\text{A}_6\text{Sn}_2\text{Se}_4(\text{PSe}_5)_2$  (A = Rb, Cs),<sup>7</sup>  $\text{Rb}_3\text{Sn}(\text{PSe}_5)(\text{P}_2\text{Se}_6)$ ,<sup>8</sup> and the quinary  $\text{Rb}_4\text{Sn}_2\text{Ag}_4\text{P}_6\text{Se}_{18}$ .<sup>9</sup> The common oxidation state of tin in chalcophosphates is 4+ because the excess chalcogen in the flux favors the higher oxidation state. Exceptions include  $\text{Sn}_2\text{P}_2\text{Q}_6$  (Q = S, Se),<sup>10</sup>  $\text{TiSnPS}_4$ ,<sup>11</sup> and  $\text{Rb}_4\text{Sn}_2\text{Ag}_4\text{P}_6\text{Se}_{18}$ ,<sup>9</sup> which feature  $\text{Sn}^{2+}$ . In this regard, it is interesting to understand the interplay between high- and lower-valent tin and how the fluxes may play a role in affecting it. Here we report the synthesis and characterization of the first examples of quaternary selenophosphate compounds featuring  $\text{Sn}^{2+}$ ,  $\text{K}_{10}\text{Sn}_3(\text{P}_2\text{Se}_6)_4$ , and  $\text{Cs}_2\text{SnP}_2\text{Se}_6$ , made by the polychalcophosphate flux method at 850 °C.<sup>12</sup>

$\text{K}_{10}\text{Sn}_3(\text{P}_2\text{Se}_6)_4$  crystallizes in the space group  $R\bar{3}$  in a new structure type.<sup>13</sup> It features a highly anionic, three-dimensional  $[\text{Sn}_3(\text{P}_2\text{Se}_6)_4]^{10-}$  framework with  $\text{K}^+$  counterions (Figure 1a).

\*To whom correspondence should be addressed. E-mail: m-kanatzidis@northwestern.edu.

(1) (a) Chung, I.; Jang, J. I.; Malliakas, C. D.; Ketterson, J. B.; Kanatzidis, M. G. *J. Am. Chem. Soc.* 2010, 132, 384. (b) Chung, I.; Song, J. H.; Jang, J. I.; Freeman, A. J.; Ketterson, J. B.; Kanatzidis, M. G. *J. Am. Chem. Soc.* 2009, 131, 2647. (c) Chung, I.; Malliakas, C. D.; Jang, J. I.; Canlas, C. G.; Weliky, D. P.; Kanatzidis, M. G. *J. Am. Chem. Soc.* 2007, 129, 14996. (d) Chung, I.; Jang, J. I.; Gave, M. A.; Weliky, D. P.; Kanatzidis, M. G. *Chem. Commun.* 2007, 4998. (e) Lacroix, P. G.; Clement, R.; Nakatani, K.; Zyss, J.; Ledoux, I. *Science* 1994, 263, 658.

(2) (a) Thompson, A. H.; Whittingham, M. S. U.S. Patent 4,049,879, 1977. (b) Lemehaute, A.; Ouvrard, G.; Brec, R.; Rouxel, J. *Mater. Res. Bull.* 1977, 12, 1191.

(3) (a) Banerjee, S.; Szarko, J. M.; Yuhas, B. D.; Malliakas, C. D.; Chen, L. X.; Kanatzidis, M. G. *J. Am. Chem. Soc.* 2010, 132, 5348. (b) Chung, I.; Song, J. H.; Kim, M. G.; Malliakas, C. D.; Karst, A. L.; Freeman, A. J.; Weliky, D. P.; Kanatzidis, M. G. *J. Am. Chem. Soc.* 2009, 131, 16303. (c) Banerjee, S.; Malliakas, C. D.; Jang, J. I.; Ketterson, J. B.; Kanatzidis, M. G. *J. Am. Chem. Soc.* 2008, 130, 12270. (d) Gauthier, G.; Jobic, S.; Boucher, F.; Macaudiere, P.; Huguenin, D.; Rouxel, J.; Brec, R. *Chem. Mater.* 1998, 10, 2341.

(4) (a) Bourdon, X.; Grimmer, A. R.; Cajipe, V. B. *Chem. Mater.* 1999, 11, 2680. (b) Scott, B.; Pressprich, M.; Willet, R. D.; Cleary, D. A. *J. Solid State Chem.* 1992, 96, 294. (c) Carpentier, C. D.; Nitsche, R. *Mater. Res. Bull.* 1974, 9, 1097.

(5) Breshears, J. D.; Kanatzidis, M. G. *J. Am. Chem. Soc.* 2000, 122, 7839.

(6) (a) Kanatzidis, M. G. *Curr. Opin. Solid State Mater. Sci.* 1997, 2, 139. (b) McCarthy, T. J.; Kanatzidis, M. G. *Chem. Mater.* 1993, 5, 1061–1063. (c) Chondroudis, K.; McCarthy, T. J.; Kanatzidis, M. G. *Inorg. Chem.* 1996, 35, 840–844. (d) Huang, S.-P.; Kanatzidis, M. G. *Inorg. Chem.* 1991, 30, 1455.

(7) Chondroudis, K.; Kanatzidis, M. G. *J. Chem. Soc., Chem. Commun.* 1996, 1371.

(8) Chondroudis, K.; Kanatzidis, M. G. *J. Solid State Chem.* 1998, 136, 79.

(9) Chondroudis, K.; Kanatzidis, M. G. *Inorg. Chem.* 1998, 37, 2848.

(10) Enjalbert, R.; Galy, J.; Vysochanskii, Y.; Ouedraogo, A.; Saint-Gregoire, P. *Eur. Phys. J. B* 1999, 8, 169.

(11) Becker, R.; Brockner, W.; Eisenmann, B. *Z. Naturforsch., A: Phys. Sci.* 1987, 42, 1309.

(12) The synthesis of  $\text{K}_{10}\text{Sn}_3(\text{P}_2\text{Se}_6)_4$  and  $\text{Cs}_2\text{SnP}_2\text{Se}_6$  was achieved by reacting a 5:3:8:19  $\text{A}_2\text{Se}/\text{Sn}/\text{P}/\text{Se}$  (A = K, Cs) mixture under a vacuum in a carbon-coated fused-silica tube at 850 °C for 3 days, followed by cooling at a rate of 2 °C/h to 300 °C. The excess flux was dissolved with degassed DMF under a  $\text{N}_2$  atmosphere to reveal red plate  $\text{K}_{10}\text{Sn}_3(\text{P}_2\text{Se}_6)_4$  crystals with the byproduct of  $\text{Sn}_2\text{P}_2\text{Se}_6$  (~20%) and pure orange thick rod  $\text{Cs}_2\text{SnP}_2\text{Se}_6$  crystals. Pure title compounds could be obtained by reacting a stoichiometric mixture of the same reagents in a fused-silica tube at 800 °C for 2 h, followed by quenching to air.

(13) Crystal data for  $\text{K}_{10}\text{Sn}_3(\text{P}_2\text{Se}_6)_4$  at 100(2) K: STOE II diffractometer, Mo K $\alpha$  radiation ( $\lambda = 0.71073$  Å), trigonal,  $R\bar{3}$ ,  $a = b = 24.1184(7)$  Å,  $c = 17.6482(2)$  Å,  $V = 3852.9(2)$  Å<sup>3</sup>,  $Z = 3$ ,  $D_c = 3.736$  g/cm<sup>3</sup>,  $\mu = 19.524$  mm<sup>-1</sup>,  $\theta_{\text{max}} = 27.50^\circ$ , 10 750 total reflections, 1960 unique reflections with  $R_{\text{int}} = 6.83\%$ , GOF = 1.209, 86 parameters,  $R1 = 3.79\%$ ,  $wR2 = 8.27\%$  for  $I > 2\sigma(I)$ . No evidence of supercell, merohedral, or nonmerohedral twinning was found.

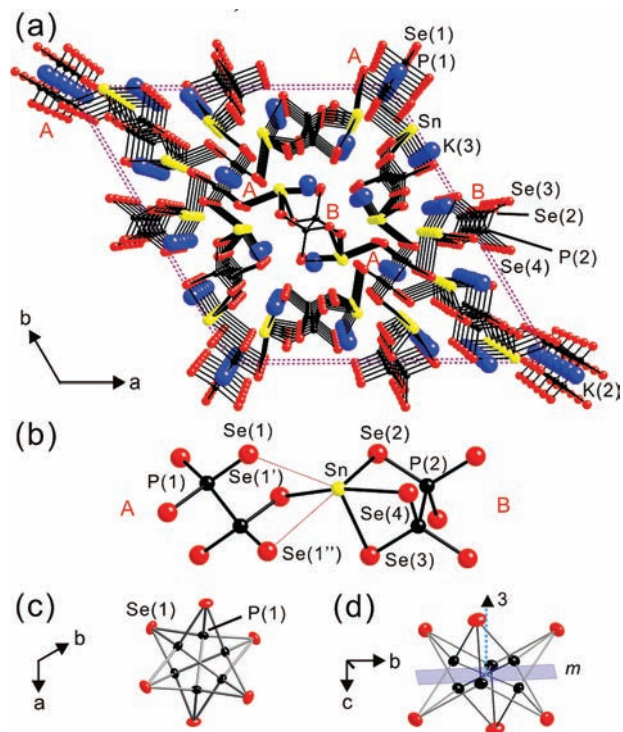


**Figure 1.** (a) Structure of  $K_{10}Sn_3(P_2Se_6)_4$  viewed down the  $c$  axis featuring a unique three-dimensional framework. Two crystallographically independent  $[P_2Se_6]^{4-}$  anions are labeled as “A” and “B”. Disordered atoms, including K(1) atoms, are removed for clarity. Color code: blue, K atoms; yellow, Sn atoms; black, P atoms; red, Se atoms. Each atom is labeled. (b) Local structure of the Sn atom. Red dotted lines represent the nonbonding interaction between Sn and Se atoms. (c and d) Orientationally disordered  $[P_2Se_6]^{4-}$  anions residing on (0 0 0.5), one of the special positions of the space group  $R\bar{3}$ , shown with thermal ellipsoids of 50% probability. A superimposed image of three  $[P_2Se_6]^{4-}$  units in different orientations that share the center of symmetry at the special position is shown. The (0 0 1) mirror plane and the crystallographic 3-fold rotation axis forcing the disorder are shown in part d.

The crystallographically unique Sn atoms are randomly disordered with K(1) atoms, and their occupancy is refined to 50%. The four-coordinate  $Sn^{2+}$  center is capped by two chelating  $[P_2Se_6]^{4-}$  units from opposite directions (Figure 1b) to form a three-dimensional framework structure. Two crystallographically unique  $[P_2Se_6]^{4-}$  units are denoted as A and B. The local geometry of the  $Sn^{2+}$  center resembles a distorted trigonal bipyramid with an empty apical position. The  $5s^2$  lone pair of  $Sn^{2+}$  appears to occupy the space, as indicated by nonbonding interactions of Sn atoms toward Se atoms of the  $[P_2Se_6]^{4-}$  (A) ligand. The distances of Sn–Se atoms of the monodentate  $[P_2Se_6]^{4-}$  (A) are relatively long at Sn–Se(1') = 3.121(7) Å, with long nonbonding contacts of  $Sn \cdots Se(1) = 3.633(6)$  Å and  $Sn \cdots Se(1'') = 3.794(9)$  Å. Those of the tridentate  $[P_2Se_6]^{4-}$  (B) ligand are shorter at Sn–Se(2) = 2.927(1) Å, Sn–Se(3) = 2.901(1) Å, and Sn–Se(4) = 2.908(5) Å. These are similar to those in  $SnSe^{14}$  and  $Sn_2P_2Se_6$ .<sup>10</sup>

The  $[P_2Se_6]^{4-}$  (A) anion adopts three different orientations (Figure 1c,d), and therefore P(1) is one-third occupied. Because the atomic sites in the unit cell are defined by symmetry elements, a structural motif therein tends to resemble the symmetry of its crystallographic position. The

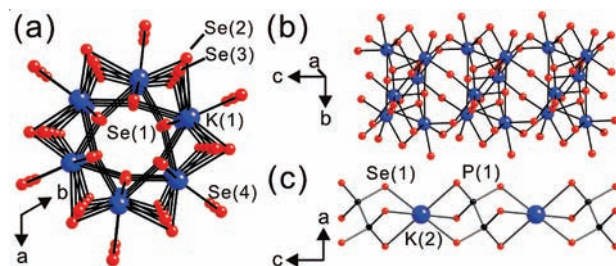


**Figure 2.** Local coordination environments of K(1) and K(2) atoms. (a and b)  $K(1)Se_8$  dodecahedra that form a one-dimensional tubular structure. (c)  ${}_1^\infty[K(2)(P_2Se_6)^{3-}]$  chain.

$[P_2Se_6]^{4-}$  (A) anion resides on the fixed-symmetry elements that they do not possess, i.e., on the special position of the trigonal space group  $R\bar{3}$ : (0 0 0.5) [Wyckoff position 3b, site symmetry  $\bar{3}$ ]. The  $[P_2Se_6]^{4-}$  anion has the  $D_{3h}$  point group when ideal, and the P–P bond of the anion is tilted with respect to the crystallographic  $c$  axis. Accordingly, the  $[P_2Se_6]^{4-}$  anions are forced to be positionally disordered by the  $\bar{3}$  symmetry operation. As a result, P and Se atoms of  $[P_2Se_6]^{4-}$  (A) appear to form their own antiprisms (Figure 1d). A similar symmetry-related disorder is found in  $Cs_{10}P_8Se_{20}$ <sup>15</sup> and  $[Mo_2Cl_8]^{n-}$ .<sup>16</sup> This disordered model was further confirmed with solid-state magic-angle-spinning (MAS)  $^{31}P$  NMR spectroscopy, which is described later.

The eight-coordinate K(1) atom is surrounded by two of each tridentate (A) and monodentate (B)  $[P_2Se_6]^{4-}$  anions in a distorted dodecahedral geometry. The  $K(1)Se_8$  dodecahedra form an infinite, one-dimensional tubular structure running down the  $c$  axis, generated by the  $\bar{3}$  symmetry operation (Figure 2a). First, three  $K(1)Se_8$  dodecahedra correlated by the 3-fold rotation on the same  $a$ – $b$  plane form a six-membered ring via corner-sharing. Then, this trimer generates itself by the  $\bar{3}$  operation just below its plane to assemble the novel hexamer cluster of  $K_6Se_{18}(\mu_3-Se_{18/3})(\mu_2-Se_{12/2})$ . Finally, the clusters condense via selenium bridges to give a nanotubular chain (Figure 2b). The K(1)–Se distances are from 3.081 to 3.348(8) and 3.858(8) Å. The K(2) atom resides at the exact middle of two  $[P_2Se_6]^{4-}$  (A) anions: the special position  $(\frac{2}{3} \frac{1}{3} \frac{1}{3})$ . It and two tridentate  $[P_2Se_6]^{4-}$  (A) anions from opposite directions condense to give an infinite one-dimensional chain running down the  $c$  axis (Figure 2c). The K(2) atom, centered at the ideal antiprismatic geometry, is coordinated by six Se(1) atoms that are generated by the  $\bar{3}$  symmetry operation. The K(2)–Se(1) distance is 3.307(5) Å. The nine-coordinate K(3) atom is surrounded by two tridentate  $[P_2Se_6]^{4-}$  (A) and three monodentate  $[P_2Se_6]^{4-}$  (B) anions, showing an irregular polyhedral geometry. The K(3)–Se distances range widely from 3.290(5) to 3.87(2) Å.

$Cs_2SnP_2Se_6$  adopts the space group  $P2_1/c$ <sup>17</sup> and features parallel infinite one-dimensional chains of  ${}_1^\infty[SnP_2Se_6^{2-}]$  separated by  $Cs^+$  cations (Figure 3a). When viewed down the (1 0 1) direction, the  ${}_1^\infty[SnP_2Se_6^{2-}]$  chains and  $Cs^+$  cations are

(15) Chung, I.; Holmes, D.; Weliky, D. P.; Kanatzidis, M. G. *Inorg. Chem.* **2010**, *49*, 3092.

(16) Cotton, F. A.; Eglin, J. L. *Inorg. Chim. Acta* **1992**, *198*–200, 13.

(17) Crystal data for  $Cs_2SnP_2Se_6$  at 100(2) K: STOE II diffractometer, Mo  $K\alpha$  radiation ( $\lambda = 0.71073$  Å), monoclinic,  $P2_1/c$ ,  $a = 10.1160(4)$  Å,  $b = 12.7867(5)$  Å,  $c = 11.0828(5)$  Å,  $V = 1429.2(1)$  Å<sup>3</sup>,  $Z = 4$ ,  $D_c = 4.277$  g/cm<sup>3</sup>,  $\mu = 22.264$  mm<sup>−1</sup>,  $\theta_{max} = 26.29^\circ$ , 10 599 total reflections, 2955 unique reflections with  $R_{int} = 6.70\%$ , GOF = 1.123, 112 parameters,  $R1 = 4.38\%$ ,  $wR2 = 7.64\%$  for  $I > 2\sigma(I)$ .

(14) Adouby, K.; Perez-Vicente, C.; Jumas, J. C.; Fourcade, R.; Toure, A. A. Z. *Kristallogr.* **1998**, *213*, 343.

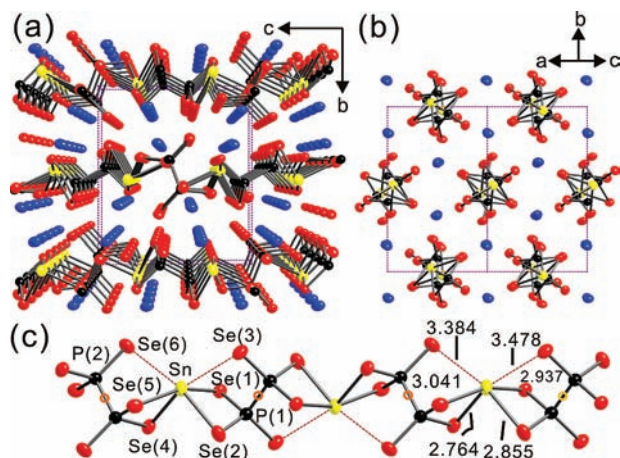


**Figure 3.** Structure of  $\text{Cs}_2\text{SnP}_2\text{Se}_6$  viewed down (a) the  $a$  axis and (b) the crystallographic  $(1\ 0\ 1)$  direction. (c) Structure, labeling, and Sn–Se distances (Å) of  $[\text{SnP}_2\text{Se}_6]^{2-}$ . Color code: blue, Cs atoms; yellow, Sn atoms; black, P atoms; red, Se atoms. Red dotted lines represent nonbonding Sn  $\cdots$  Se interactions. Orange circles centered at P–P bonds show the center of symmetry. The thermal ellipsoids: 90% probability.

hexagonally packed (Figure 3b). The crystallographically unique  $\text{Sn}^{2+}$  center is coordinated by two different, chelating bidentate  $[\text{P}_2\text{Se}_6]^{4-}$  units from opposite directions to form the single chain of  $[\text{SnP}_2\text{Se}_6]^{2-}$  (Figure 3c). There is a crystallographic center of symmetry dictating 2-fold rotation at the center of the P–P bonds. Accordingly, the  $5s^2$  lone pair electrons of Sn point up and down, alternating along the chain direction. The Sn–Se distances are normal at 2.764(1), 2.855(1), 2.937(1), and 3.041(1) Å, with two long nonbonding interactions at 3.384(2) and 3.478(1) Å. The structure of  $\text{Cs}_2\text{SnP}_2\text{Se}_6$  is related to that of  $\text{A}_2\text{MP}_2\text{Se}_6$  ( $A = \text{K}, \text{Rb}, \text{Cs}$ ;  $M = \text{Mn}, \text{Fe}$ ).<sup>18</sup>

$\text{K}_{10}\text{Sn}_3(\text{P}_2\text{Se}_6)_4$  and  $\text{Cs}_2\text{SnP}_2\text{Se}_6$  were synthesized by the same reaction profile: reacting a mixture of 5:3:8:19  $\text{A}_2\text{Se}/\text{Sn}/\text{P}/\text{Se}$  ( $A = \text{K}, \text{Cs}$ ) at 850 °C for 3 days, followed by cooling at a rate of 2 °C/h to 300 °C. Note that the complex three-dimensional structure of  $\text{K}_{10}\text{Sn}_3(\text{P}_2\text{Se}_6)_4$  is broken into the simpler one-dimensional structure of  $\text{Cs}_2\text{SnP}_2\text{Se}_6$  as the flux basicity increases (i.e., with a bigger alkali metal). A more basic flux or higher reaction temperature tends to give shorter structural fragments.<sup>19</sup> The  $\text{K}^+$  salt formed with  $\text{Sn}_2\text{P}_2\text{Se}_6$  (~20%), whereas the  $\text{Cs}^+$  salt was phase pure after washing with *N,N*-dimethylformamide (DMF). Pure title compounds could be obtained by the direct combination reaction at 800 °C for 2 h, followed by quenching in air (Supporting Information, Figure S1). Flux reactions with  $\text{Li}_2\text{Se}$  and  $\text{Na}_2\text{Se}$  gave mainly  $\text{Sn}_2\text{P}_2\text{Se}_6$  because of the weak basicity of the smaller alkali metals.  $\text{K}_{10}\text{Sn}_3(\text{P}_2\text{Se}_6)_4$  is stable in DMF, alcohol, formamide, acetonitrile, and air but decomposed in deionized  $\text{H}_2\text{O}$  to give a hazy red solution. The compound is soluble in *N*-methylformamide, forming a clear yellow solution.  $\text{Cs}_2\text{SnP}_2\text{Se}_6$  is insoluble in these organic solvents and deionized  $\text{H}_2\text{O}$  and is stable in air.

According to differential thermal analysis performed at a rate of 10 °C/min,  $\text{K}_{10}\text{Sn}_3(\text{P}_2\text{Se}_6)_4$  and  $\text{Cs}_2\text{SnP}_2\text{Se}_6$  melt

congruently at 538 and 573 °C, and the melts crystallize at 547 and 595 °C, respectively (Supporting Information, Figure S2). The powder X-ray diffraction patterns before and after melting/recrystallization were identical for both compounds.

The  $^{31}\text{P}$  NMR spectrum of  $\text{K}_{10}\text{Sn}_3(\text{P}_2\text{Se}_6)_4$  (Supporting Information, Figure S3) collected at a 14 kHz MAS frequency revealed a single isotropic chemical shift at 36.3 ppm, indicating a unique P-containing structural motif in the compound. The result supports the disordered model of the  $[\text{P}_2\text{Se}_6]^{4-}$  (A) anion, and  $[\text{P}_2\text{Se}_6]^{4-}$  (A and B) anions are locally and magnetically equivalent. A similar result was reported for  $\text{Cs}_{10}\text{P}_8\text{Se}_{20}$ , including the positionally disordered  $[\text{P}_2\text{Se}_6]^{4-}$  anion. The chemical shift value is close to those of  $\text{Pb}_2\text{P}_2\text{Se}_6$ <sup>20</sup> (29.1 ppm) and  $\text{Sn}_2\text{P}_2\text{Se}_6$ <sup>21</sup> (29.7 ppm), which have a similar  $[\text{P}_2\text{Se}_6]^{4-}$  unit. The solid-state optical absorption spectra of  $\text{K}_{10}\text{Sn}_3(\text{P}_2\text{Se}_6)_4$  and  $\text{Cs}_2\text{SnP}_2\text{Se}_6$  (Supporting Information, Figure S4) reveal well-defined absorption edges and band gaps of 1.82 and 2.06 eV, respectively, which are in good agreement with their red/orange color.

Raman spectra of  $\text{K}_{10}\text{Sn}_3(\text{P}_2\text{Se}_6)_4$  and  $\text{Cs}_2\text{SnP}_2\text{Se}_6$  are active, with shifts at 144, 162, 175, 220, 424, 444, and 472  $\text{cm}^{-1}$  for the former and 181, 215, 252, 442, and 473  $\text{cm}^{-1}$  for the latter (Supporting Information, Figure S5). By comparison to  $\text{Sn}_2\text{P}_2\text{Se}_6$ , the shifts below 200  $\text{cm}^{-1}$  account for the external modes and internal Se–P–Se bending modes and those from 400 to 500  $\text{cm}^{-1}$  are related to P–Se valence vibrations.<sup>22</sup> The peaks at 215 and 220  $\text{cm}^{-1}$  can be unambiguously assigned to the locally  $A_{1g}$  symmetric stretching mode of the  $\text{P}_2\text{Se}_6$  unit.<sup>1b</sup> The far-IR spectra showed peaks at 194, 225, 253, 301, 438, 445, 484, and 496  $\text{cm}^{-1}$  for  $\text{K}_{10}\text{Sn}_3\text{P}_8\text{Se}_{24}$  and 179, 201, 230, 299, 405, 450, 484, and 521  $\text{cm}^{-1}$  for  $\text{Cs}_2\text{SnP}_2\text{Se}_6$ , similar to those of compounds that possess  $[\text{P}_2\text{Se}_6]^{4-}$  anions<sup>23</sup> (Supporting Information, Figure S6).

The results of this study demonstrate that the lower oxidation state of  $\text{Sn}^{2+}$  can be stabilized by the polychalcophosphate flux method at high temperature. Presumably, the oxidation chemistry of  $\text{Sn}^{2+}$  by Se–Se bonds in the flux, favored at lower temperatures, is inhibited at higher temperatures. The strong dependence of the structure and composition on the alkali metal highlights the rich chalcogenide chemistry of tin and the important role of the flux basicity.

**Acknowledgment.** Financial support was provided by the National Science Foundation (Grant DMR-0801855).

**Supporting Information Available:** X-ray crystallographic file (in CIF format), experimental details, crystallographic refinement data, powder X-ray diffraction, differential thermal analysis, and solid-state MAS  $^{31}\text{P}$  NMR, optical absorption, Raman, and FT-IR spectroscopy data. This material is available free of charge via the Internet at <http://pubs.acs.org>.

(20) Canlas, C. G.; Kanatzidis, M. G.; Weliky, D. P. *Inorg. Chem.* **2003**, *42*, 3399.

(21) Francisco, R. H. P.; Tepe, T.; Eckert, H. J. *Solid State Chem.* **1993**, *107*, 452.

(22) van Loosdrecht, P. H. M.; Maior, M. M.; Molnar, S. B.; Vysochanskii, Y. M.; van Bentum, P. J. M.; van Kempen, H. *Phys. Rev. B* **1993**, *48*, 6014.

(23) Kliche, G. J. *Solid State Chem.* **1984**, *51*, 118.

(18) McCarthy, T. J.; Kanatzidis, M. G. *Inorg. Chem.* **1995**, *34*, 1257.

(19) Kanatzidis, M. G.; Sutorik, A. C. *Prog. Inorg. Chem.* **1995**, *43*, 151.